Gazi University Journal of Science
GU J Sci
23(3):327-338 (2010)

GUJS
www.gujs.org

Finite Element Analysis of Finite Strain Elastoplastic Contact-Impact Problems

Ahmet Erklig[1♠], Ibrahim H. Guzelbey[1], Abdulkadir Cevik[2]

[1]*University of Gaziantep, Mechanical Engineering Department, 27310, Gaziantep, Turkey*
[2]*University of Gaziantep, Civil Engineering Department, 27310, Gaziantep, Turkey*

Received: 26.08.2009 Revised: 02.12.2009 Accepted: 02.12.2009

ABSTRACT

In this study a finite element analysis of elastoplastic contact-impact has been carried out. Newmark, Wilson-θ, Central Difference and Houbolt Methods have been used as direct integration methods. Impact analysis includes elastoplastic and large deformation based upon updated Lagrangian including buckling check. The results show that the direct integration methods give different results due to different contact-impact cases. Plastic analysis is more stable than the elastic analysis.

Keywords: Elastoplastic Contact-Impact, Finite Element Analysis, Direct Integration Methods, Finite Strain

1. INTRODUCTION

The solution of elastoplastic finite strain contact-impact problems requires a transient analysis using some numerical methods called as direct integration methods [1-3]. Direct integration methods are based on two approaches. The first approach is to satisfy the equilibrium equation at time intervals Δt. In the second approach, a variation of displacements, velocities, and accelerations in a time interval Δt is assumed. Velocities and accelerations are approximated in terms of displacements based on finite difference expressions. In each method, a different finite difference approximation is used to predict the velocity and acceleration for each time interval. The well-known dynamic equation is given as follows:

$$\underline{M}\,\ddot{\underline{\delta}} + \underline{C}\,\dot{\underline{\delta}} + \underline{K}\,\underline{\delta} = \underline{F} \qquad (1)$$

where $\underline{\delta}$, $\dot{\underline{\delta}}$, $\ddot{\underline{\delta}}$ and $\underline{F}$ are displacement, velocity, acceleration and force vectors. $\underline{M}$, $\underline{K}$ and $\underline{C}$ are the mass, damping, and stiffness matrices [4]. The equation (1) is solved using the direct integration methods such as Newmark, Wilson-θ, Central Difference and Houbolt Methods.

A finite strain elastoplastic contact-impact problem is a highly non-linear problem due to geometry, material and boundary conditions. These non-linearities can be handled using a finite strain elastoplastic analysis in the solution algorithm. This solution algorithm has been designed for impact problems considering the contact and buckling analysis based upon finite element approach. Algorithm contains the incremental elastoplastic finite strain procedure in each time increment. Each time increment also contains elastoplastic contact analysis, large deformation and buckling check in direct integration methods. This solution algorithm has been shown in the preceeding sections. The related components of this algorithm have also been given in finite strain elastoplastic contact-impact analysis section.

In this study, an attempt has been made to investigate the transient analysis of finite-strain elastoplastic contact-impact problems using Finite Element Method (FEM). Algorithms have been tested for some contact-impact cases. Buckling check has also been included in the algorithm for further studies.

♠Corresponding author, e-mail: erklig@gantep.edu.tr

2. FINITE STRAIN ELASTOPLASTIC CONTACT-IMPACT ANALYSIS

Updated Lagrangian Approach has been used in this study for finite strain analysis. Elastoplastic equations are adapted for finite strain analysis [4, 5, 6].

2.1.1. Finite Strain Elastoplastic Equations

Consider an engineering structure in equilibrium under an initial mechanical loading. Applying a virtual displacement, then the following equation is obtained according to the principle of virtual work:

$$d\chi = dU - dW = 0 \tag{2}$$

where $d\chi$, dU and dW represent the variations of total potential energy, strain energy and work done by external force, due to the applied virtual displacement. An equivalent nodal force vector $\underline{F}$ may be defined such that:

$$dW = d\underline{\delta}^t \underline{F} \tag{3}$$

where $d\underline{\delta}$ represents the variation of the nodal displacement vector, and the strain energy can be expressed as follows:

$$dU = \iiint_{\Omega} d\underline{\varepsilon}^t \, \underline{\sigma} \, dxdydz \tag{4}$$

where Ω represents the domain of the component. Displacement components can be interpolated over each finite element, and it is possible to derive a matrix $\underline{B}$ such that:

$$d\underline{\varepsilon} = \underline{B} d\underline{\delta} \tag{5}$$

over every finite element. If the domain Ω is discretised into *n* finite elements, then the equation (4) may be rewritten as follows:

$$dU = d\underline{\delta}^t \left[\sum_{e=1}^{n} \iiint_{\Omega_e} \underline{B}^t \underline{\sigma} \, dx \, dy \, dz \right] \tag{6}$$

Substituting from equation (3) and (6) into (2), then it can be shown that:

$$d\chi = d\underline{\delta}^t \left[\sum_{e=1}^{n} \iiint_{\Omega_e} \underline{B}^t \underline{\sigma} \, dx \, dy \, dz - \underline{F} \right] = 0 \tag{7}$$

Since Equation (7) is valid for any arbitrary virtual displacement, then, it can be deduced that:

$$\sum_{e=1}^{n} \iiint_{\Omega_e} \underline{B}^t \underline{\sigma} \, dx \, dy \, dz - \underline{F} = 0 \tag{8}$$

which represents the generalized equation of equilibrium.

From the definition of Green's strain tensor, the engineering strain components for two-dimensional problems may be expressed in terms of the following form:

$$\underline{\varepsilon} = \underline{\varepsilon}_S + \underline{\varepsilon}_L \tag{9}$$

where

$$\underline{\varepsilon} = \left\{ \varepsilon_x \;\; \varepsilon_y \;\; \gamma_{xy} \right\}$$

and $\underline{\varepsilon}_S$ represents the Cauchy's strain vector and $\underline{\varepsilon}_L$ represents the high order terms in Green's strain components [4, 5]. The variation of the above vectors can be expressed in terms of displacement components (u, v) and their variations as follows.

$$d\underline{\varepsilon}_S = \begin{bmatrix} \dfrac{\partial du}{\partial x} \\ \dfrac{\partial dv}{\partial y} \\ \dfrac{\partial du}{\partial y} + \dfrac{\partial dv}{\partial x} \end{bmatrix} \tag{10}$$

and

$$d\underline{\varepsilon}_L = \begin{bmatrix} \left(\dfrac{\partial u}{\partial x}\right)\left(\dfrac{\partial du}{\partial x}\right) + \left(\dfrac{\partial v}{\partial x}\right)\left(\dfrac{\partial dv}{\partial x}\right) \\ \left(\dfrac{\partial u}{\partial y}\right)\left(\dfrac{\partial du}{\partial y}\right) + \left(\dfrac{\partial v}{\partial y}\right)\left(\dfrac{\partial dv}{\partial y}\right) \\ \left(\dfrac{\partial u}{\partial x}\right)\left(\dfrac{\partial du}{\partial y}\right) + \left(\dfrac{\partial u}{\partial y}\right)\left(\dfrac{\partial du}{\partial x}\right) + \left(\dfrac{\partial v}{\partial x}\right)\left(\dfrac{\partial dv}{\partial y}\right) + \left(\dfrac{\partial v}{\partial y}\right)\left(\dfrac{\partial dv}{\partial y}\right) \end{bmatrix} \tag{11}$$

Defining a slope vector $\underline{\theta}$ such that:

$$\underline{\theta} = \left\{ \frac{\partial u}{\partial x} \;\; \frac{\partial v}{\partial x} \;\; \frac{\partial u}{\partial y} \;\; \frac{\partial v}{\partial y} \right\} \tag{12}$$

then equation (11) may be rewritten as follows:

$$d\underline{\varepsilon}_L = \underline{A} d\underline{\theta} \equiv d\underline{A} \;\; \underline{\theta} \tag{13}$$

where

$$\underline{A} = \begin{bmatrix} \dfrac{\partial u}{\partial x} & \dfrac{\partial v}{\partial x} & 0 & 0 \\ 0 & 0 & \dfrac{\partial u}{\partial y} & \dfrac{\partial v}{\partial y} \\ \dfrac{\partial u}{\partial y} & \dfrac{\partial v}{\partial y} & \dfrac{\partial u}{\partial x} & \dfrac{\partial v}{\partial x} \end{bmatrix} \tag{14}$$

Writing displacement components at any point inside an element in terms of nodal values and shape functions, i.e.

$$u(x,y) = \sum_i u_i N_i(\xi,\eta) \;\text{ and }\; v(x,y) = \sum_i v_i N_i(\xi,\eta) \tag{15}$$

where N_i represents Lagrangian shape functions in terms of intrinsic coordinates ξ, η, then it can be proved that:

$$d\underline{\varepsilon}_S = \underline{B}_S d\underline{\delta} \tag{16}$$

$$d\underline{\theta} = \underline{G} d\underline{\delta} \tag{17}$$

$$d\underline{\varepsilon}_L = \underline{A}\ \underline{G}\, d\underline{\delta} = B_L d\underline{\delta} \tag{18}$$

where

$$\underline{B}_S = \begin{bmatrix} \cdots & \dfrac{\partial N_i}{\partial x} & 0 & \cdots \\ \cdots & 0 & \dfrac{\partial N_i}{\partial y} & \cdots \\ \cdots & \dfrac{\partial N_i}{\partial y} & \dfrac{\partial N_i}{\partial x} & \cdots \end{bmatrix} \tag{19}$$

and

$$\underline{G} = \begin{bmatrix} \cdots & \dfrac{\partial N_i}{\partial x} & 0 & \cdots \\ \cdots & 0 & \dfrac{\partial N_i}{\partial x} & \cdots \\ \cdots & \dfrac{\partial N_i}{\partial y} & 0 & \cdots \\ \cdots & 0 & \dfrac{\partial N_i}{\partial y} & \cdots \end{bmatrix} \tag{20}$$

$$\underline{B}_L = \underline{A}\ \underline{G} \tag{21}$$

Hence, it can be deduced from equations (5), (9), (16) and (18) that:

$$\underline{B} = \underline{B}_S + \underline{B}_L \tag{22}$$

Notice also that, the variation of the $\underline{B}$ matrix due to a virtual displacement is:

$$d\underline{B} = d\underline{B}_L \tag{23}$$

and the total strain vector is:

$$\underline{\varepsilon} = \int_{\underline{0}}^{\underline{\delta}} \left(\underline{B}_S + \underline{B}_L\right) d\underline{\delta} = \left(\underline{B}_S + \frac{1}{2}\underline{B}_L\right)\underline{\delta} \tag{24}$$

Generally speaking, equation (8) represents a non-linear system of equations. If an approximate solution is found, in terms of $\underline{\delta}$, $\underline{\sigma}$, $\underline{B}$ then:

$$\underline{R} = \underline{F} - \sum_e \iiint_{\Omega_e} \underline{B}^t\, \underline{\sigma}\, dxdydz \tag{25}$$

represents the residual force vector from such an approximation. If the exact solution is represented by

$$\underline{\sigma}_{ex} = \underline{\sigma} + \Delta\underline{\sigma} \tag{26}$$

$$\underline{B}_{ex} = \underline{B} + \Delta\underline{B} \tag{27}$$

then from Eq. (8):

$$\sum_e \iiint_{\Omega_e} \left(\underline{B} + \Delta\underline{B}\right)^t \left(\underline{\sigma} + \Delta\underline{\sigma}\right) dxdydz - \underline{F} = \underline{0}$$

i.e. by neglecting $\Delta\underline{B}^t \Delta\underline{\sigma}$ term:

$$\sum_e \left[\iiint_{\Omega_e} \underline{B}^t \Delta\underline{\sigma}\, dxdydz + \iint_{\Omega_e} \Delta\underline{B}^t \underline{\sigma}\, dxdydz \right] \approx \underline{R} \tag{28}$$

The value of $\Delta\underline{\sigma}$ may be approximated as follows:

$$\Delta\underline{\sigma} = \underline{D}_t\, \Delta\underline{\varepsilon} = \underline{D}_t\, \underline{B}\, \Delta\underline{\delta} \tag{29}$$

where $\underline{D}_t$ may represent a tangential stress-strain matrix, and $\underline{D}_t = \underline{D}_{ep}$ for elastoplastic analysis.

The term $\Delta\underline{B}^t \Delta\underline{\sigma}$ may be simplified as follows:

$$\Delta\underline{B}^t \underline{\sigma} = \Delta\underline{B}_L^t\, \underline{\sigma} = \underline{G}^t \Delta\underline{A}\ \underline{\sigma} \text{ i.e. } \Delta\underline{B}^t \underline{\sigma} = \underline{G}^t \underline{S}\ \underline{G}\ \Delta\underline{\delta} \tag{30}$$

where

$$\underline{S} = \begin{bmatrix} \sigma_x & 0 & \tau_{xy} & 0 \\ 0 & \sigma_x & 0 & \tau_{xy} \\ \tau_{xy} & 0 & \sigma_y & 0 \\ 0 & \tau_{xy} & 0 & \sigma_y \end{bmatrix} \tag{31}$$

Using equations (29) and (30), then equation (28) may be rewritten in the following matrix form:

$$(\underline{K}_t + \underline{K}_\sigma)\Delta\underline{\delta} = \underline{R} \tag{32}$$

where

$$\underline{K}_t = \sum_e \iiint_{\Omega_e} \underline{B}^t \underline{D}\underline{B}\, dx\, dy\, dz \tag{33}$$

$$\underline{K}_\sigma = \sum_e \iiint_{\Omega_e} \underline{G}^t \underline{S}\ \underline{G} dx\, dy\, dz \tag{34}$$

Equation (32) represents the linearised finite element equations of equilibrium, and an iterative algorithm is required in order to obtain an accurate solution.

2.1.2. Finite-Element Finite Strain Elastoplastic Solution Algorithm

The suggested solution algorithm has been introduced based upon initial stress approach [5]. For this purpose, consider a complex structure, at an initial state of equilibrium under a force $\underline{F}_0$, with displacement, stress and strain vectors being $\underline{\delta}_0$, $\underline{\sigma}_0$ and $\underline{\varepsilon}_0$. Applying a force increment $\Delta\underline{F}$, the following algorithm may be employed to find the corresponding accurate answers with finite strain elastoplasticity taken into consideration.

a) Initial Calculations:

(i) From equation (32), the finite element equations required to be solved are:

$$\left(\underline{K}_0+\underline{K}_\sigma\right)\Delta\underline{\delta}_0=\Delta\underline{F}$$

where

$$\underline{K}_0=\sum_e\iiint_{\Omega_e}\underline{B}_0^t\left(\underline{D}_{ep}\right)_0\underline{B}_0\,dxdydz$$

$$\underline{K}_\sigma=\sum_e\iiint_{\Omega_e}\underline{G}^t\underline{S}_0\underline{G}\,dxdydz$$

The matrix $\underline{B}_0$ is defined as follows:

$$\underline{B}_0=\underline{B}_S+\underline{B}_L\left(\underline{\delta}_0\right)$$

and $\underline{D}_{ep}$, $\underline{S}_0$ matrices are based upon ($\underline{\sigma}_0,\underline{\varepsilon}_0$). Hence

$$\underline{\delta}_1=\underline{\delta}_0+\Delta\underline{\delta}_0$$

(ii) Calculate the corresponding strain increment $\Delta\underline{\varepsilon}'$, from

$$\Delta\underline{\varepsilon}^t{}_0=\int_{\underline{\delta}_0}^{\underline{\delta}_1}\underline{B}d\underline{\delta}=\underline{B}_S\Delta\underline{\delta}_0+\frac{1}{2}\underline{B}_L\left(\underline{\delta}_1\right)\underline{\delta}_1-\frac{1}{2}\underline{B}_L\left(\underline{\delta}_0\right)\underline{\delta}_0$$

The corresponding stress increment is

$$\Delta\underline{\sigma}'_0=\left(\underline{D}_{ep}\right)_0\Delta\underline{\varepsilon}'$$

b) Elastoplastic Stress-Strain Corrections:

If the total stress at any point has not exceeded the yield point of the material, then: $\Delta\varepsilon_o=\Delta\underline{\varepsilon}_o^t$ and $\Delta\sigma_o=\Delta\underline{\sigma}_o^t$ otherwise $\Delta\varepsilon_o=\Delta\underline{\varepsilon}_o^t$ and the initial-stress approach is used to find the corrected stress increment $\Delta\underline{\sigma}_0$, Hence

$$\underline{\varepsilon}_1=\underline{\varepsilon}_0+\Delta\underline{\varepsilon}_0 \text{ and } \underline{\sigma}_1=\underline{\sigma}+\Delta\underline{\sigma}_0$$

The residual force vector is obtained as follows:

$$\Delta\underline{R}_1=\Delta\underline{F}-\sum_e\iiint_{\Omega_e}\left[\underline{B}_S^t+\underline{B}_L^t\left(\underline{\delta}_1\right)\right]\Delta\underline{\sigma}\,dxdydz$$

c) r[th] Iteration, r=1,2,..

(i) Find updated $\underline{D}_r$, $\underline{S}_r$, $\underline{B}_r$ such that:

$$\underline{D}_r=\underline{D}_{ep}\left(\underline{\sigma}_r,\underline{\varepsilon}_r\right)$$

$$\underline{S}_r=\underline{S}\left(\underline{\sigma}_r\right)$$

$$\underline{B}_r=\underline{B}_S+\underline{B}_L\left(\underline{\delta}_r\right)$$

(ii) Hence find the corresponding stiffness matrices:

$$\underline{K}_r=\sum_e\iiint_{\Omega_e}\underline{B}_r^t\,\underline{D}_r\,\underline{B}_r\,dxdydz$$

$$\underline{K}_\sigma=\sum_e\iiint_{\Omega_e}\underline{G}^t\underline{S}_r\underline{G}\,dxdydz$$

Notice that, in the modified Newton-Raphson scheme, $\underline{D}_r$ is taken as the elastic stress-strain matrix and $\underline{B}_r$ is replaced by the $\underline{B}_S$ matrix.

(iii) Solve

$$(\underline{K}_r+\underline{K}_\sigma)\Delta\underline{\delta}_r=\Delta\underline{R}_r$$

then find:

$$\underline{\delta}_{r+1}=\underline{\delta}_r+\Delta\underline{\delta}_r \text{ and } (\underline{B}_L)_{r+1}=\underline{B}_L\left(\underline{\delta}_{r+1}\right)$$

(iv) Calculate the corresponding strain increment:

$$\Delta\underline{\varepsilon}_r=\underline{B}_S\Delta\underline{\delta}_r+\frac{1}{2}\left[\left(\underline{B}_L\right)_{r+1}\underline{\delta}_{r+1}-\left(\underline{B}_L\right)_r\underline{\delta}_r\right]$$

(v) Calculate non-corrected stress increment

$$\Delta\grave{\underline{\sigma}}_r=\underline{D}_r\Delta\underline{\varepsilon}_r \quad \underline{\varepsilon}_{r+1}=\underline{\varepsilon}_r+\Delta\underline{\varepsilon}_r \quad \grave{\underline{\sigma}}_{r+1}=\underline{\sigma}_r+\Delta\grave{\underline{\sigma}}_r$$

(vi) Use elastic-plastic initial-stress approach to find the corrected stress increment $\Delta\underline{\sigma}_r$, hence:

$$\underline{\sigma}_{r+1}=\underline{\sigma}_r+\Delta\underline{\sigma}_r$$

(vii) The new residual force vector is:

$$\Delta\underline{R}_{r+1}=\underline{F}-\sum_e\iiint_{\Omega_e}\underline{B}_{r+1}^t\underline{\sigma}_{r+1}\,dxdydz$$

where

$$\underline{F}=\underline{F}_0+\Delta\underline{F}$$

(viii) Find the following convergence measures:

$$\underline{\varepsilon}_\delta=\frac{\Delta\underline{\delta}_r^t\,\Delta\underline{\delta}_r}{\underline{\delta}_{r+1}^t\,\underline{\delta}_{r+1}} \text{ and } \underline{\varepsilon}_F=\frac{\Delta\underline{R}_{r+1}^t\,\Delta\underline{R}_{r+1}}{\underline{F}^t\underline{F}}$$

and stop the iteration if the value of each of them is less than a given permissible value.

2.1.3. Nonlinear Buckling Analysis

There are two nonlinearities in the large deflection problems. The first one is the strain-displacement equations. The second comes from the equilibrium equations. In the solution algorithm, these are taken into account at each step.

A linearized stability analysis is convenient from a mathematical viewpoint but quite restrictive in practical applications. It is required to determine the nonlinear load-deflection behavior of a structure. Two approaches:have evolved for determining load deflection beahviour of the structure: incremental and iterational

methdos. In the incremental method, the load is applied as small increments so that the structure can be assumed to respond linearly during each increment. For each increment of load, increments of displacements and corresponding stress and strain are computed. A subsequent increment of load is applied and the process is continued until the desired number of increment. This part has been included in algorithm. In this method, it can be possible to obtain a reasonable results and convergence if a suitably small increment of load is choosen. Nonlinear buckling analysis has been included in algorithm for further studies (see Figure 1).

2.1.4. Contact, Impact and Release Condition

For an incremental contact algorithm, contact zones are discretised in terms of a system of pairs of surface or interface elements. Each pair has the first element with nodes on the first surface whilst the second element has nodes on the second surface. In flexible contact, each pair of the interface elements should have matching nodes. Whenever the contact occurs, interface elements will be remeshed. So the coordinates of every pair of nodes in contact will be same. In each load increment, the nodal coordinates are updated. Load should be applied in proportional increments. If X_l is defined as the load ratio, then the load increment becomes;

$$\Delta \underline{F} = \underline{X}_l \underline{F} \tag{35}$$

where $\underline{F}$ is the total loading vector, which includes prescribed tractions or displacements.

According to the characteristics of the problem the load increment can be applied fully or in terms of subincrements. If the subincrements are used, load increment becomes

$$(\Delta \underline{F})_j = \alpha_j \underline{X}_i \underline{F} \tag{36}$$

where $\sum \alpha = 1$.

To prevent nodes becoming in contact or separation with more than one node during loading the subincrements must be adjusted automatically. All the nodes in contact zones are checked so as to find a value of α which brings the nearest node to contact or separate. A new load subincrement $\alpha \Delta \underline{F}$ will be applied if the value of α is acceptable (i.e. $\sum \alpha \le 1$). When $|\alpha| < \alpha$ permissible value, then the nearest value has come into contact or separation, and a modification for the BCs should be carried out before applying the next subincrement. The total previous value can be used to start the next subincrement, which led to a change to BCs, unless: $\sum \alpha > 1$ and the value of final load ratio is determined for such case as $\sum \alpha = 1$ and then, no more modification is done [7]. When impacting body touches to target with a velocity, contact is considered to be started. Until contact forces turn to the negative, deformation carries on. Contact forces and elastic buckling are checked at each time increment. Once contact forces equal to negative value, then release is started. Contact BCs of related FE nodes are released. When all contacting nodes have negative forces, impacting body leaves the target [8]. This procedure has been given in Figure 1.

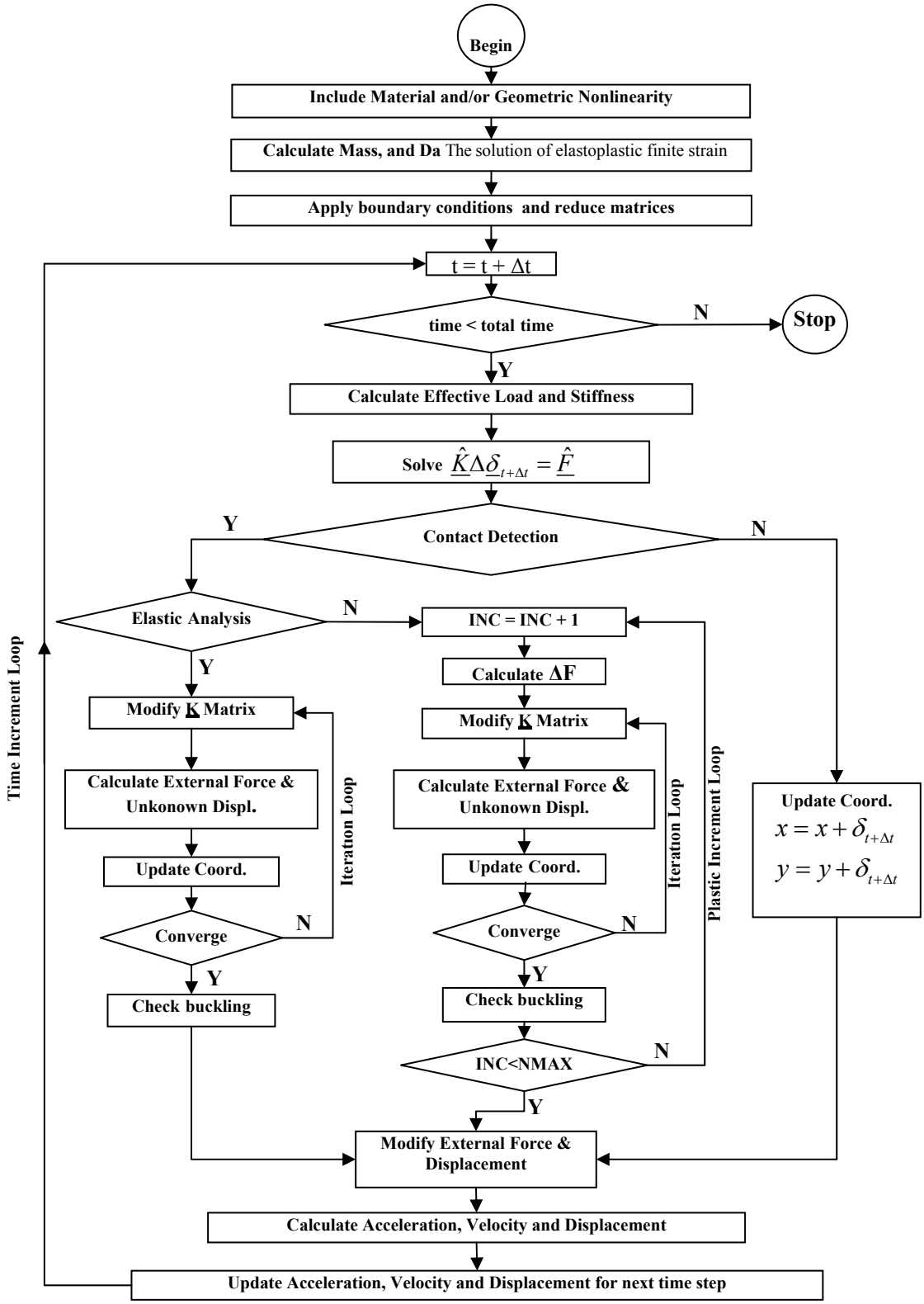

Figure 1. General Solution Algorithm for Finite strain Elastoplastic Contact-Impact

3. CASE STUDIES AND DISCUSSION

3.1. Impact of conical-end rectangular bar

Conical end rectangular bar with initial velocity V=0.5 m/sec collides with a fixed rectangle block, as shown in Figure 2. For simplicity, the bar and block have been selected from the same material. Material properties of the rectangular bar and block are: $\rho = 1000$ kg/m^3, E = 5000 Pa, $\nu = 0.3$ and $\sigma_y = 500$ Pa

The FE model has 115 4-noded rectangular elements, as shown in Figure 3. Time increment is taken as $\Delta t = 0.001$ sec. The deformations, velocities and stresses of contact point and deformation of whole model have been given in Figure 4-13 for elastic and plastic analysis.

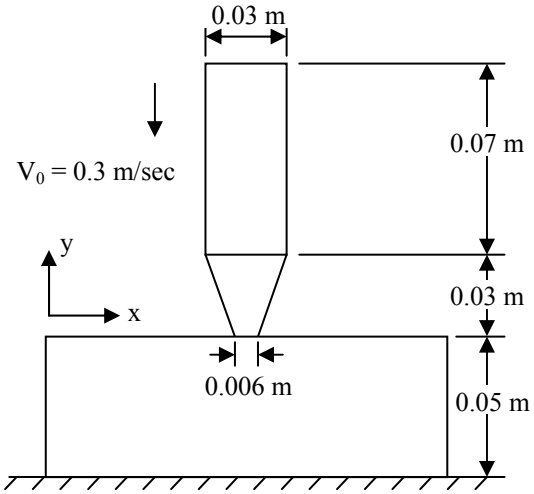

Figure 2. Impact of conical end rectangular bar

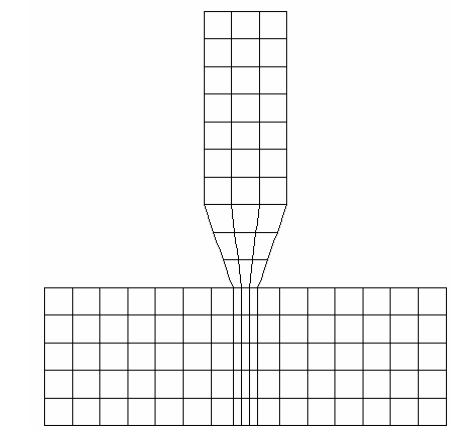

Figure 3. FE model of conical end rectangular bar

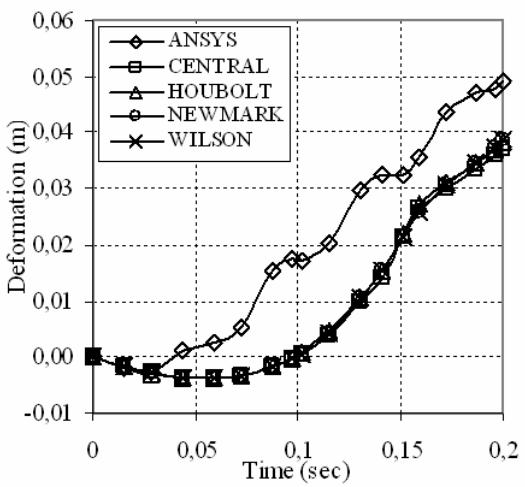

Figure 4 Vertical deformation at contact point of the conical end rectangular bar for elastic analysis

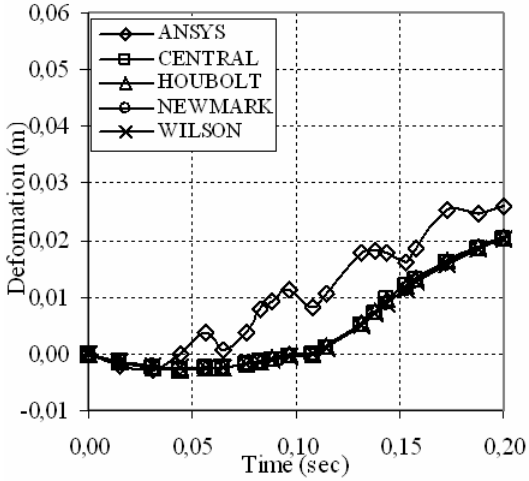

Figure 5 Vertical deformation at contact point of the conical end rectangular bar for elastoplastic analysis

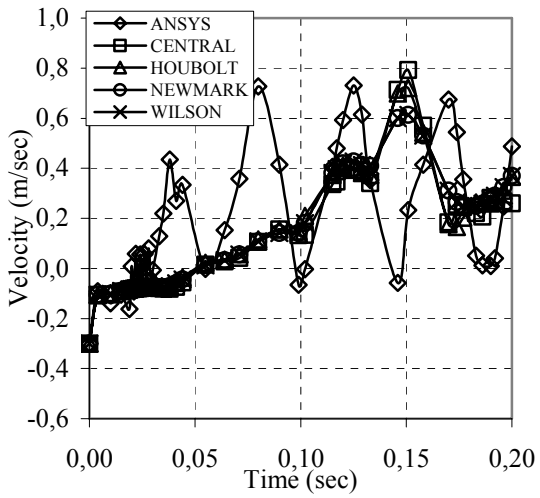

Figure 6 Vertical velocity at contact point of the conical end rectangular bar for elastic analysis

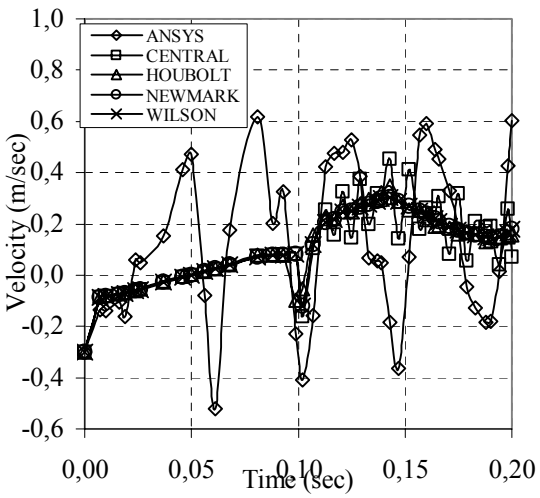

Figure 7 Vertical velocity at contact point of the conical end rectangular bar for elastoplastic analysis

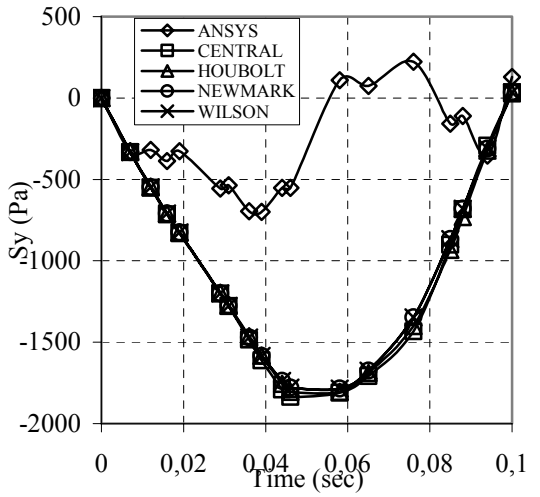

Figure 8. Vertical stress at contact point of the conical rectangular bar for elastic analysis.

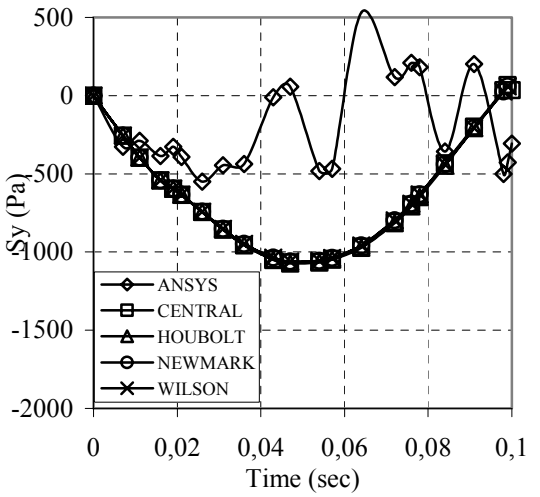

Figure 9. Vertical stress at contact point of the end conical end rectangular bar for elastoplastic analysis.

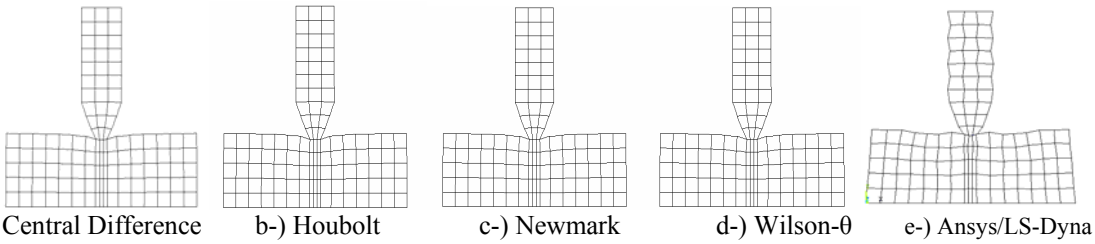

Figure 10. Deformation of the conical end rectangular bar at time t=0.06 sec (Elastic Analysis).

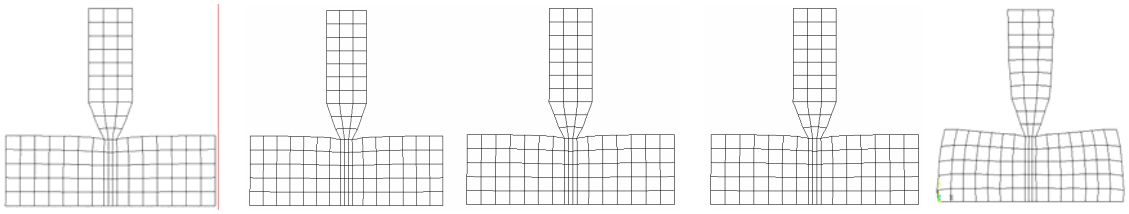

Figure 11. Deformation of the conical end rectangular bar at time t=0.06 sec (Elastoplastic Analysis).

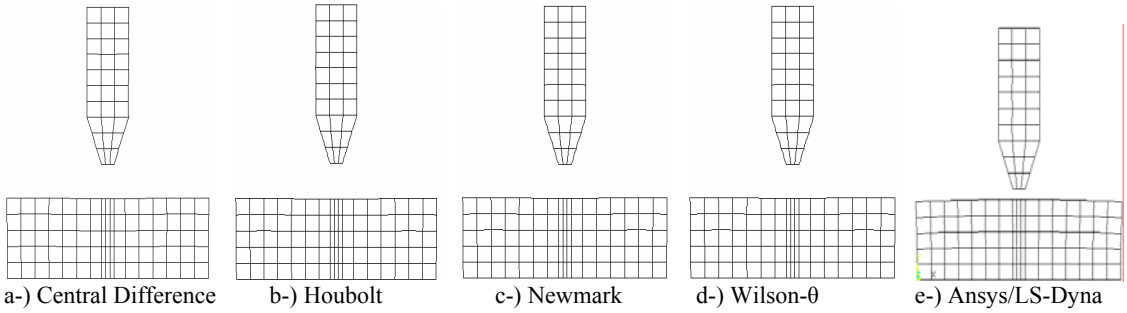

Figure 12. Deformation of the conical end rectangular bar at time t=0.15 sec (Elastic Analysis).

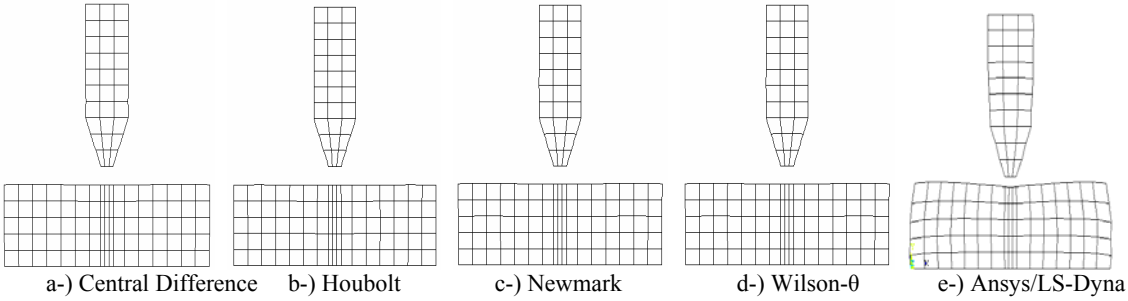

Figure 13. Deformation of the conical end rectangular bar at time t=0.15 sec (Elastoplastic Analysis).

3.2. Impact of ball

In this case round-end rectangular bar with initial velocity V=0.5 m/sec collide with the fixed block as shown in Figure 14. Same material properties are used as in previous case. The FE mesh with 182 4-noded rectangular elements is shown in Figure 15. The time increment $\Delta t = 0.001$ sec is employed. The deformations, velocities and stresses of contact point and deformation of whole model have been given in Figure 16-25 for elastic and plastic analysis.

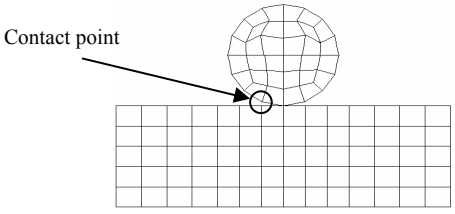

Figure 15 FE mesh of the ball

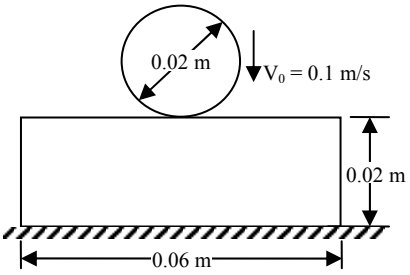

Figure 14 Impact of a ball with initial velocity

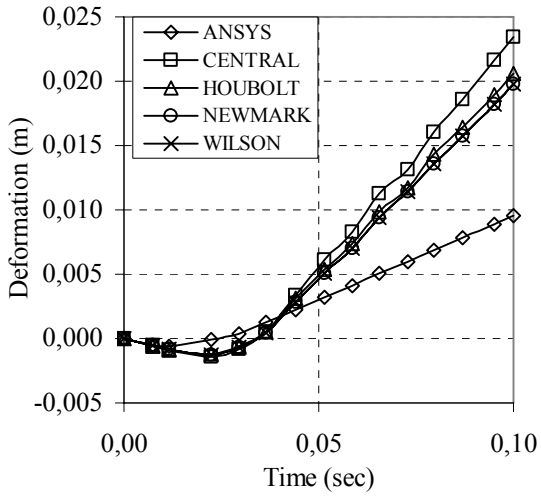

Figure 16 Vertical deformation at contact point of the ball for elastic analysis

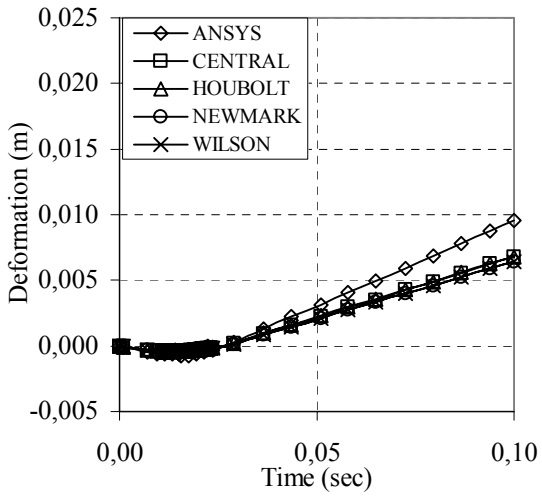

Figure 17 Vertical deformation at contact point of the ball for elastoplastic analysis

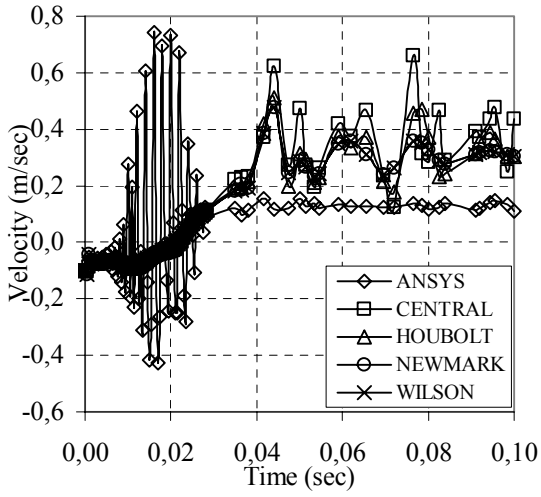

Figure 18 Vertical velocity at contact point of the ball for elastic analysis

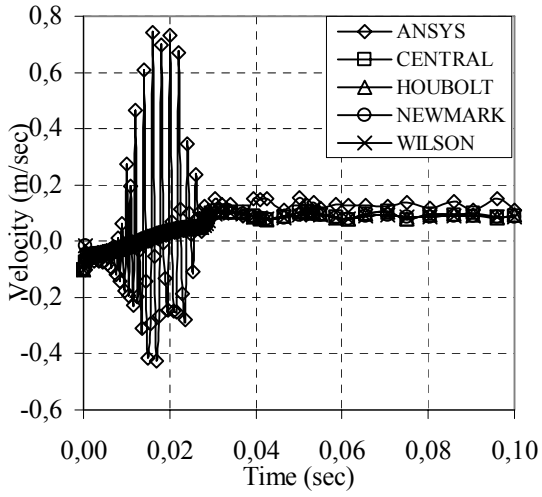

Figure 19 Vertical velocity at contact point of the ball for elastoplastic analysis

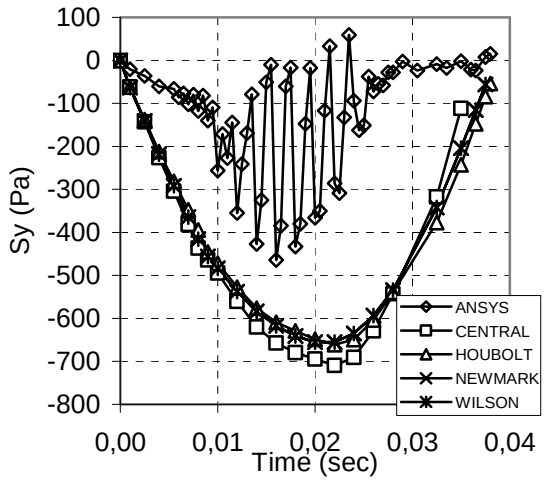

Figure 20 Vertical stress at contact point of elastic analysis

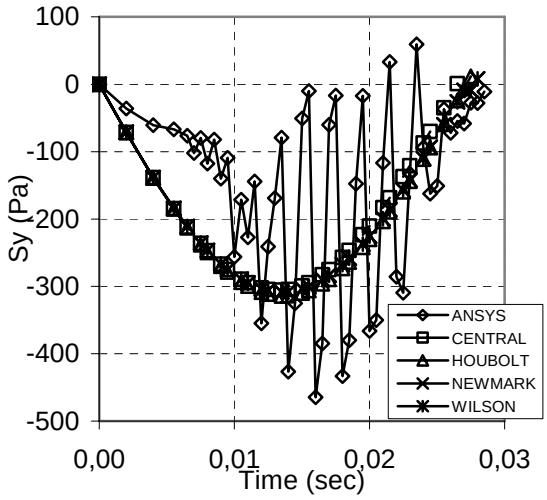

Figure 21 Vertical stress at contact point ofthe ball for the ball for elastoplastic analysis

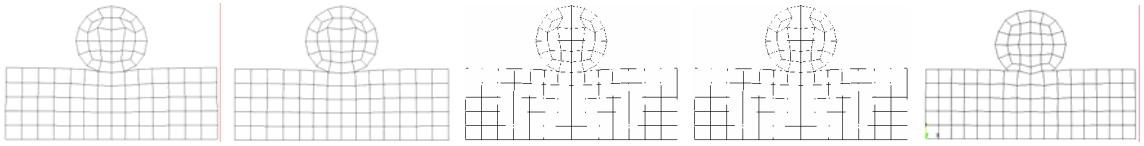

a-) Central Difference b-) Houbolt c-) Newmark d-) Wilson-θ e-) Ansys/LS-Dyna

Figure 22 Deformation of the ball at time t=0.024 sec (Elastic Analysis)

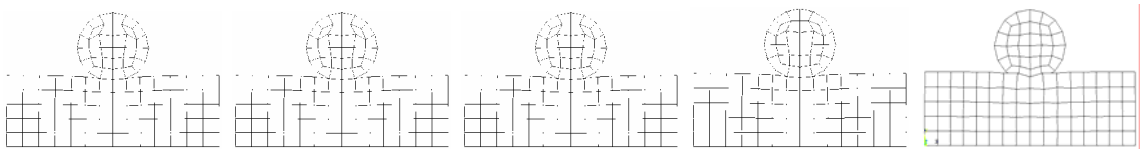

a-) Central Difference b-) Houbolt c-) Newmark d-) Wilson-θ e-) Ansys/LS-Dyna

Figure 23 Deformation of the ball at time t=0.024 Sec (Elastoplastic Analysis)

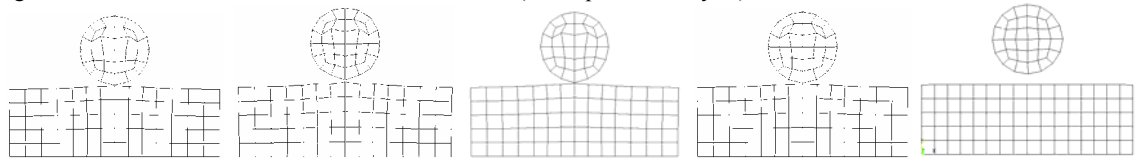

a-) Central Difference b-) Houbolt c-) Newmark d-) Wilson-θ e-) Ansys/LS-Dyna

Figure 24 Deformation of the ball at time t=0.1 sec (Elastic Analysis)

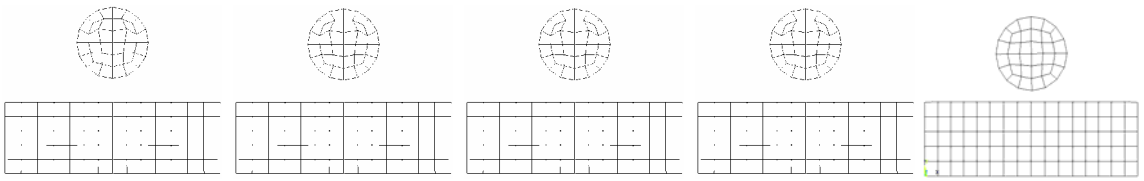

a-) Central Difference b-) Houbolt c-) Newmark d-) Wilson-θ e-) Ansys/LS-Dyna

Figure 25 Deformation of the ball at time t=0.1 Sec (Elastoplastic Analysis)

4. DISCUSSION

Case studies prove that the developed program has a stable solution algorithm. Non-conforming contact is very accurate and stable for developed programs but ANSYS/LS-DYNA has large fluctuations due to iteration number, time increment and number of element. But conforming contact results follow the same trend with ANSYS/LS-DYNA.

Generally, plastic solutions are more stable than elastic solutions. For conforming and nonconforming contact impact cases, deformation, velocity and stress have been examined against to ANSYS/LS-DYNA with same increment and iteration number used in developed program. The most important advantage of ANSYS/LS-DYNA is the automatic time and load increment algorithm for the non-linear problems, which adjusts itself due to outcoming results.

This stability of plastic analysis results in the developed program is due to designed algorithm. As it is expected, the values of the displacement, velocity and stress of the plastic cases are smaller than the values of elastic cases due to dissipated energy. Hence the plastic analysis of conforming and non-conforming contact is very stable when they are compared with elastic case.

Deformation: For conforming contact cases, central difference and Houbolt deformation results are better than Newmark and Wilson-θ direct integration methods. But, Newmark and Wilson-θ are better than central difference and Houbolt for non-conforming contact cases. However, they gave quite similar results with each other and trace the same trend with ANSYS/LS-DYNA.

Velocity: Newmark and Wilson-θ are more stable than central difference and Houbolt methods. Among them, central difference gave the worst result. This difference is related with the formulations of methods. In spite of the fluctuation of velocity in central difference, it still follows the same trend of the other methods. Moreover, four direct integration methods gave similar results with ANSYS/LS-DYNA.

Stress: Generally, all the methods gave similar results. But there is an important difference between four direct integration methods and ANSYS/LS-DYNA due to using the same iteration number, time increment and element size in the developed program's cases. However ANSYS/LS-DYNA's results close to the developed program's results when the iteration number, time increment and number of element are increased.

The results and the accuracy of the direct integration methods mostly depend upon the case and parameter, which have been considered. This result is due to the formulation of these methods. Central difference is an explicit method but all of the three are implicit methods.

5. CONCLUSIONS

Generally, all the direct integration methods gave quite acceptable results. Due to case and parameter (deformation, velocity and stress), they have some differences. Newmark and Wilson-θ methods are quite stable for non-conforming contact. Houbolt method is moderate but Central Difference is less accurate for the non-conforming contact case. However, Central Difference delivers better result for conforming contact.

The developed program gave better results than ANSYS/LS-DYNA for the non-conforming contact cases. But the contact algorithm requires a further improvement for conforming contact case. Finite strain elastoplastic algorithm is accurate and stable.

REFERENCES

[1] Bathe K.J. and Wilson E.L., "Numerical methods in finite element analysis", Prentice-Hall, NY (1976).

[2] Zienkiewicz O.C., "The finite element methods in engineering 2nd ed.", Mc Graw-Hill, London (1971).

[3] Chen W.H., Yeh J.T., "Three-dimensional finite element analysis of static and dynamic contact problems with friction", Comp. & Struc., 35(5): p541-552 (1990).

[4] Erklig A., "Finite element analysis of finite strain elasto-plastic impact problems", Ph.D Thesis, University of Gaziantep, Gaziantep, Türkiye (2003).

[5] Guzelbey I.H., "Finite and boundary element analysis of elasto-plastic finite strain contact problems", Ph.D Thesis, Cranfield Institute of Technology, UK (1992).

[6] Owen D.R.J. and Hinton E., "Finite elements in plasticity: theory and practice", Pineridge Press (1980).

[7] Kanber B, Guzelbey I.H. and Erklig A., "Boundary element analysis of contact problems using artificial boundary node approach", Acta Mech Sinica, 19 (4): 347-354 (2003).

[8] Guzelbey I. H., Erklig A. and Kanber B. „The efficiency of direct integration methods in elastic contact-impact problems", Acta Mech Sinica, 21: 395-401(2005).